The 15th International Symposium on Magnetic Bearings, August 3-6, 2016, Mojiko Hotel, Kitakyushu, Japan

ISMB15

Commissioning of Off-Shore Gas Compressor with 9-Axes Magnetic Bearing System: Controller Design

Beat AESCHLIMANN*, Michael HUBATKA*, Michael Ernst PETER*, Robert STETTLER* and Reza HOUSSEINI*

*Mecos AG, Industriestrasse 26, 8404 Winterthur, Switzerland

E-mail: beat.aeschlimann@mecos.com

Abstract

This paper presents the system model, model validation, controller design and test measurements for an industrial 9-axes oil-free integrated motor-compressor (tandem HOFIM™) manufactured by MAN Diesel & Turbo (MAN) to be installed off-shore on an oil rig. The magnetic bearing controller of such machines must be designed with high robustness due to large expected uncertainties in the control plant. In addition, the magnetic bearings must have a high force slew rate, and thus a high dynamic controller, since compressor surge that causes high alternating process forces cannot always be avoided in field operation. These two requirements are conflicting and it is a difficult task to find a good compromise. This paper presents an application of robust controller design and a solution to this problem: the LQG/LTR method, well described in literature, is applied for the design of the position controller. Using the proposed method, the compressor was successfully commissioned at the MAN test facility and all specifications were met.

Keywords: Oil-Free High Speed Compression, Plant Uncertainties, Compressor Surge, Model-Based Controller Design, LQG/LTR.

1. Introduction

Oil-free natural gas compressors featuring magnetic bearings are being applied more and more in the Oil&Gas industry. In the past most of the applications were mid- and downstream where the requirements for machine and bearings are benign with regard to temperature, pressure, erosion and corrosion. With increased reliability these machines are now also deployed upstream, closer to the oil well; on off-shore platforms and subsea, hundreds of meters below the water surface [1]. MAN Diesel & Turbo (MAN) is a leading supplier of high-speed integrated motor-compressors.

The tandem HOFIM™ compressor (High-Speed, Oil-Free, Integrated Motor-Compressor) consists of a central electric motor onto which two multi-stage centrifugal compressor units are attached on both sides. The individual motor and two compressor shafts are directly connected to each other and form a combined single rotor. The total rotor length and mass of the present machine is approximately 6 m and 3.5 tons. The machine is equipped with four radial active magnetic bearings (AMB) and one thrust active magnetic bearing and therefore, an AMB system with nine actively controlled axes. The two radial bearings next to the motor are called motor bearings, the two radial bearings at the ends of the shaft are called compressor bearings.

The electric motor and the magnetic bearings are cooled by the process gas (natural gas) and realize a compact machine design with several advantages, (a) there is no need for shaft seals and makes the rotor shorter, (b) stiff shaft connections provide advantageous rotordynamic behavior [2], and (c) reduced machine footprint size. Figure 1 shows an illustration of a 3D model of the compressor system.

The compact machine design introduces some challenges too. The flexible rotor dynamically couples the separate bearing planes and thus rotor balancing becomes more challenging. Furthermore, the coupled control plant for the magnetic bearing

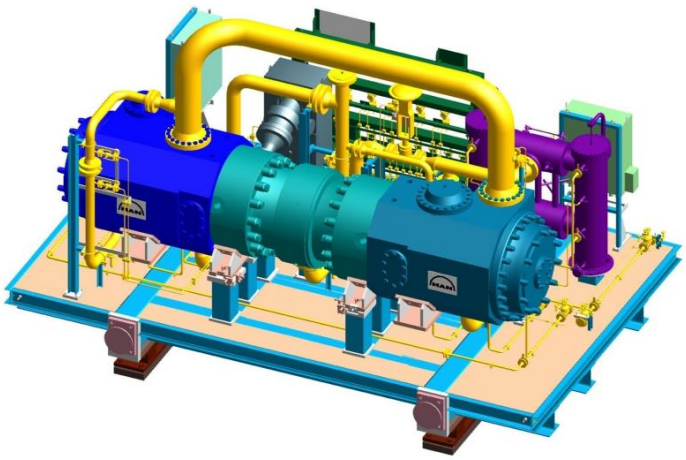

Fig. 1: Tandem HOFIM compressor (picture by MAN)

controller requires more attention in the controller design. Upstream turbo compressor application requires more stringent magnetic bearing controller requirements: High humidity content in the gas (wet gas) can lead to compressor fouling. Sour gas can attack and deteriorate bearing laminations and coil components. The above listed aspects can affect the dynamics of the control plant and in order to maintain system stability the AMB controller must be designed with a high robustness margin [5].

Model-based robust controller design offers a framework to address these challenges. Plant dynamics and couplings are inherently contained in the model used to compute the AMB controller. Cross-coupling effects in the labyrinth seals and compressor fouling can be incorporated in the controller design. The resulting controller is a fully coupled MIMO controller because the control plant itself is coupled too. The attainable performance of MIMO controllers is superior to SISO controllers. However, the implementation of MIMO controllers requires more hardware computation power and advanced software. All nine axes of the present AMB system are controlled by a single control cabinet featuring advanced MIMO control action.

Section 2 describes an analysis of the system model of the tandem HOFIM™ compressor used for the controller synthesis. In section 3 the specifications for the control system are discussed and in section 4 the applied controller design method is described. Special attention is given to the chosen model extensions and weights used for the synthesis. The compressor has been commissioned and tested in the test facility of MAN Diesel & Turbo. The performance and robustness of the controller from section 4 is evaluated and discussed.

2. System Model

In this analysis only the model of the radial control plant is considered, the modelling and controller design for the thrust bearings is not covered. The complete system model consists of the rotor model, the labyrinth seal dynamic coefficients, the negative stiffness of the motor, the sensor model, the model of the power amplifier and a model of the actuators.

The rotor is modelled with the rotordynamics code developed in the author's company. It consists of 132 beam elements for the shaft and 12 lumped masses, at the corresponding nodes, to model the compressor impellers. There are four force input stations at the locations of the magnetic bearings and four displacement output stations at the locations of the radial sensors. Additionally, there are input and output stations to introduce forces by the labyrinth seals and the electric motor. Figure 2 shows a plot of the rotor and Table 1 lists the first critical speeds modes of the rotor.

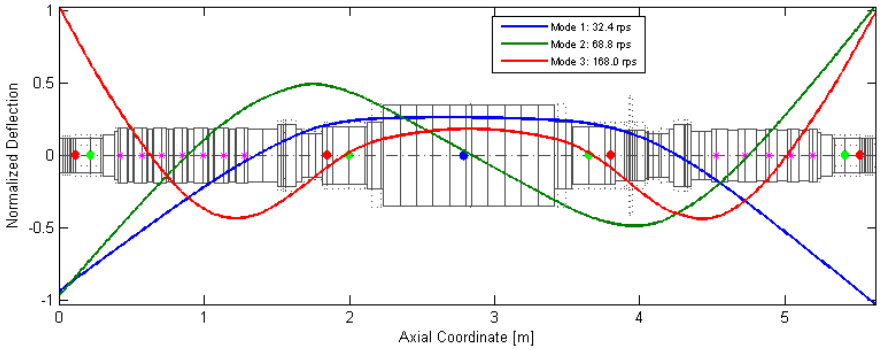

Fig. 2: Rotor model and critical speeds.

Table 1: Critical speeds and model parameters.

Critical speed 1	32.4	rps
Critical speed 2	68.8	rps
Critical speed 3	168.0	rps
Max. continuous speed	133.8	rps
Modal damping typically	0.5	%

Before building up the complete system model, the rotor model is exported as mass, gyroscopic and stiffness matrices (MGK matrix form) and transformed into modal coordinates. At this step modal damping is introduced. An initial value of 0.5% was assumed.

Labyrinth seal forces f_i along the shaft are modelled by stiffness matrices $D_{laby,i}$ and $K_{laby,i}$ provided by MAN for actual suction pressure and different rotation speeds. The motor's negative stiffness $K_{s,m}$ is concentrated at the motor center.

A number of model components introduce high frequency dynamics. The dominant dynamics of the position sensor is the anti-aliasing filter in the signal processing path. The low-pass filter is of order six with a phase loss of only 44 Degrees at 1000 Hz. The relevant component in the power amplifier is the LC output filter with a cutoff frequency of 10 kHz and a Notch filter with the same notch frequency. In Fig.3 a comparison of model and measurement is given. In order to reduce the complexity only the singular value plot is shown. The match of Eigenfrequencies and the effect of damping can be seen in the plot. The modal damping of higher modes (> 300 Hz) is underestimated by the model. This is due to additional damping effect by the high pressure surrounding gas which is not taken into account in the model. However, since the model is used for controller design a more robust design will result if the model underestimates damping.

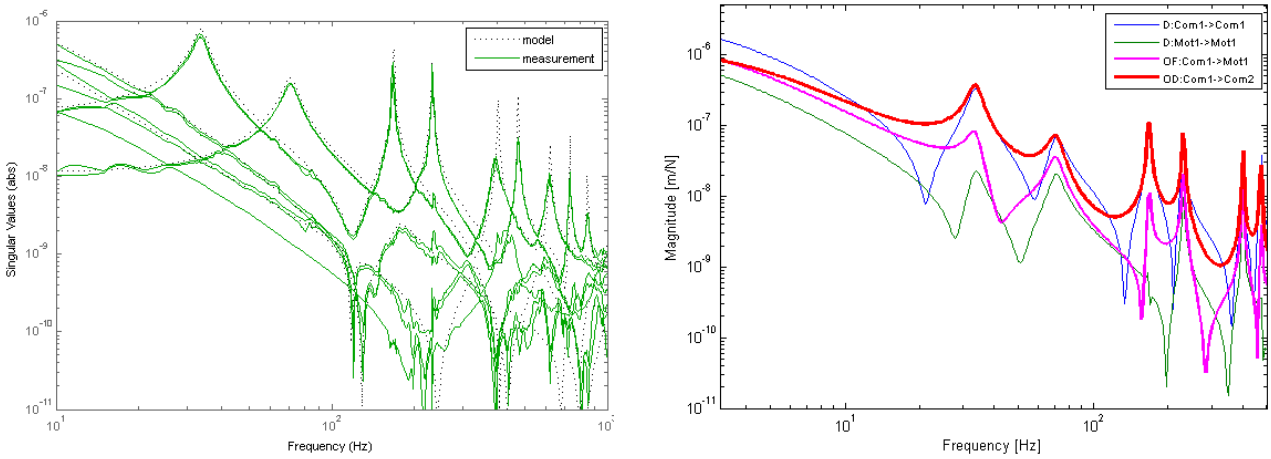

Fig. 3: Left: Singular values of model and measurement. Right: Model of the control plant. Diagonal elements compressor bearing 1 (blue) and motor bearing 1 (green) and off-diagonal elements representing the coupling between compressor bearing 1 to motor bearing 1 (magenta) and the coupling between the two compressor bearings (red).

The model can be used to study the strong dynamical couplings in the MIMO control plant. Fig. 3 shows the magnitude of two main diagonal elements of the plant; the compressor and motor bearings, and two off-diagonal elements representing the coupling between compressor bearing 1 and motor bearing 1 and the coupling between the two compressor bearings. Note in Fig. 3 that the off-diagonal elements are large and in some frequency ranges are larger than the diagonal elements. Such strong couplings in the control plant confirm the motivation to use a MIMO controller so that they can be properly taken into account and compensated.

3. Specification for the Control System

a) Nominal stability: An obvious requirement that the nominal control system must be stable at all rotation speeds.

b) Robustness: In the previous section a model of the control system with weakly damped Eigenmodes was presented. Not all model parameters are accurately known and have certain uncertainty. Furthermore, there are several reasons why the plant dynamics may even change during the lifespan of the compressor. Examples are changes in suction pressure, gas composition, and compressor fouling (deposition of micro-particles) that can cause modified seal dynamic coefficients. The position controller of the magnetic bearings must be able to maintain stability under the influence of such plant uncertainties. The ISO standard 14839, part 3, addresses this robustness issue and imposes limits on the peak values of the output sensitivity function *Se*. The standard recommends that the diagonal elements of *Se* have a peak value below 3 for newly commissioned machines.

c) Performance: Fulfilling ISO14839 does not guarantee high performance of the closed-loop (e.g. small rotor orbits, good disturbance rejection). Other criteria must be introduced. Here the dynamic compliance (*Gf*) is used: The relation between the rotor displacement and an external force input must be as low as possible for all frequencies. This is equivalent to the requirement to have good force disturbance rejection. The dynamic compliance can be seen as the inverse of the closed-loop stiffness of the AMB system. In the contrary to the specification for *Se*, no absolute upper limit ε for the compliance can be given, since the unit is m/N and therefore the upper limit depends on the range of the bearing force. The main specifications for the control system can be summarized as follows:

nominal stability

$$\max_{\omega} \left| Se(i,i,j\omega) \right| \le 3 \quad i = 1..9 \quad \text{(all diagonal elements of } Se\text{)} \tag{1}$$

$$\left|G_f(j\omega)\right| \le \varepsilon \quad \forall\omega \qquad (\varepsilon \text{ as small as possible}) \tag{2}$$

4. Controller Design

The model from section 3 is a linear state-space model of order 132. In this section this model is used to design a model based, robust position controller.

Since the singular values of a matrix are depending on the scaling of input and output signals, it is important to properly scale the inputs and outputs of the plant before controller design [5]. For a magnetic bearing system the bearing force is limited and therefore the maximum bearing force is used as input scaling W_u. On the other hand the rotor displacement is limited by the touchdown bearings and thus the touchdown bearing gaps are used for the output scaling W_y. The unscaled plant model G_{p0} from section 2 is scaled according to Eq. (3).

$$G_p(s) = W_y \setminus G_{p0} G_{int}(s) W_u \tag{3}$$

where $G_p(s)$ is the scaled plant model and G_{int} is the integrating part of the position controller. It is considered as a part of the plant during controller design. The state-space matrices A, B and C of the scaled plant are defined by Eqs. (4).

$$\dot{x}(t) = Ax(t) + Bu(t) \quad x(t) \in R^{132}, u(t) \in R^8 \tag{4}$$

$$y(t) = Cx(t) \quad y(t) \in R^8$$

$$G_p(s) = C(sI - A)^{-1} B$$

The LQG/LTR (Linear Quadratic Gaussian / Loop Transfer Recovery) method involves two basic steps [6]. In a first step (the loop-shaping step) a full state-feedback regulator is designed. In the second step (loop transfer recovery step) a state observer is appended to the control system.

4.1 Step 1: Loop-Shaping

Since the LQ regulator has a priori good robustness we have chosen it for the first step. The controller gain matrix G of the LQ regulator problem is obtained by:

$$G = \mu^{-1} B^T K(\mu) \tag{5}$$

where K is the solution of the algebraic matrix Riccati equation:

$$A^T K + KA^T - \frac{1}{2\beta} KBB^T K + Q_{mod} = 0 \tag{6}$$

The parameters are the scalar $\mu > 0$, the scalar $\beta > 1$ and the weighting matrix Q_{mod}. μ is the bandwidth parameter; smaller values of μ lead to higher bandwidth of the LQ regulator system. β is a robustness enhancement parameter. It increases the phase and gain margins of the loop-shaping LQ regulator system. The matrix Q_{mod} is the penalty matrix of the state. It contains a penalty term of the form $C^T C$ to bound the plant output, but it also contains terms to penalty directly the states of the plant, which are in fact modal coordinates. This is extremely useful to affect a particular rotor mode e.g. increase damping of a mode.

4.2 Step 2: Loop Transfer Recovery

The second step of LQG/LTR is the design of a Kalman filter such that the resulting control system meets all the specifications chosen in the first step. Therefore the second design step is also called loop transfer recovery step because it preserves the robustness and performance of the LQ regulator system. The observer gain matrix H is obtained by Eq. (7):

$$H = \Sigma(\rho) C^T \rho^{-1} \tag{7}$$

where Σ is the solution of the algebraic matrix Riccati equation Eq. (8).

$$A\Sigma + \Sigma A^T - \Sigma C^T \rho^{-1} C\Sigma + BB^T = 0 \tag{8}$$

The important LTR parameter is ρ. Smaller values of ρ yield improved recovery and larger singular values of the loop

transfer matrix. Hence ρ is chosen sufficiently small such that the singular values meet the specifications. The resulting compensator *K(s)* is given by

$$K(s) = W_u G(sI - A + BG + HC)^{-1} H / W_y \tag{9}$$

and it is of high order. Therefore an order reduction is conducted before uploading the controller to the magnetic bearing controller. For the present application a maximum controller order of 80 has been used. In Fig. 4 the sensitivity functions computed by using the model $G_p(s)$ and the compensator *K(s)* are shown.

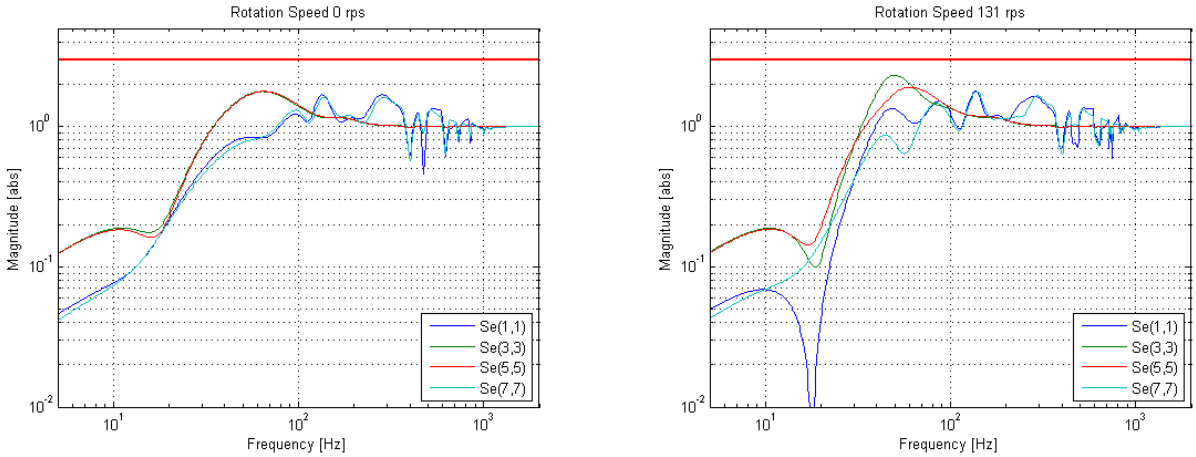

Fig. 4: Diagonal elements of computed (by using the model) sensitivity functions at standstill (left) and 131 rps (right). The red horizontal line indicates the ISO14839 upper limit

5. Test Results

The controller designed in the previous section has been tested on the real machine in the MAN test facility. The compressor system was installed in a closed gas loop with a throttle valve and heat exchangers to remove the heat from the gas after compression. The two compressor sections LP and HP are operated in serial mode. The 10 MW power was provided by a VFD. During the test runs the process gas was a mixture of Nitrogen and Helium matching the physical properties of natural gas. Fig. 5 shows a picture of the compressor during installation in the test facility.

During the commissioning the machine was accelerated stepwise to maximum continuous speed (MCS). At several different rotational speeds measurements of relevant control signals and frequency domain measurements of the control plant and the sensitivity *Se* were conducted. This exercise ensured that the control system was stable at any rotation speed. If necessary, the physical parameters of the model were adjusted to match the measurements and with the optimized model the position controller can be further improved.

A single controller was sufficient to stabilize the rotor from zero to full speed. No speed-dependent switching, except the standard UFRC/UFCC control mode, was necessary.

Figure 6 shows the measured sensitivity functions *Se* at standstill and at Maximum Continuous Speed (MCS). Under rotation the peak sensitivity is slightly higher than at standstill, especially around the gain crossover frequency. The peak at 130 Hz is a measurement artefact due to the rotation speed and is therefore not a stability problem. However, the peak values of all diagonal elements at both rotation speeds are below 3: The closed-loop thus has high overall robustness against plant uncertainties and falls into zone A, according to ISO14839 [3].

Fig. 5: Installation of HOFIM compressor in the test bed (picture by MAN).

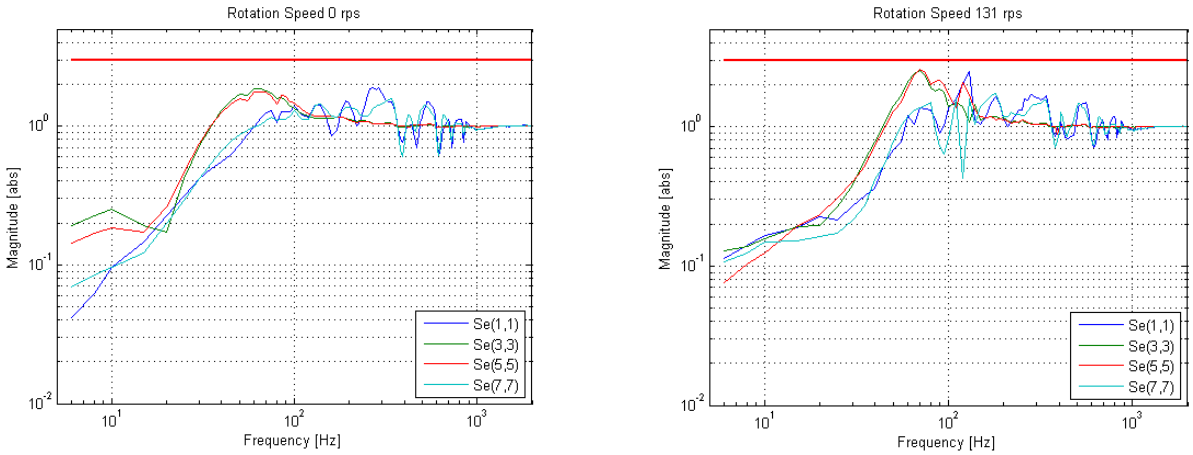

Fig. 6: Diagonal elements of measured sensitivity functions at standstill (left) and 131 rps (right). The red horizontal line indicates the ISO14839 upper limit.

The measured dynamic compliances are given in the next plot. The maximum values of the dynamic compliance lie between 30 and 70 Hz. At these frequencies the response of the rotor to external forces is highest. The achieved values have been accepted by the end customer.

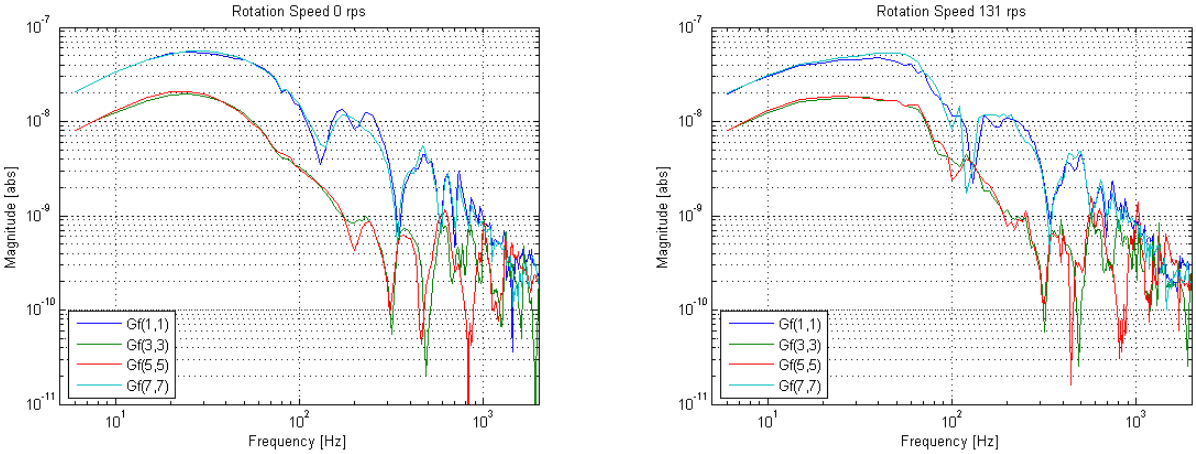

Fig. 7: Diagonal elements of measured dynamic compliance functions at standstill (left) and 131 rps (right).

Following the initial commissioning of the magnetic bearings MAN performed a series of test runs including mechanical system tests, compressor performance test and customer acceptance tests. All tests could be fulfilled successfully without the need for retuning the magnetic bearings controller. Operation of the compressor beyond the surge line revealed satisfactory dynamic behavior of the overall system. The rotor displacement from the center positions in all sensor planes, and at all rotation speeds (orbits) during factory acceptance test, fulfilled not only API617 requirements [4] but also MAN's internal, more severe specification.

6. Conclusion and Outlook

After completion of all factory acceptance tests the compressor is now being installed at the customer site, an off-shore oil rig, where the final commissioning will take place. During this final commissioning, and throughout the compressor's lifespan, the controller must prove its good robustness properties and it will be interesting to analyze the long-term variation of the control system. These long-term results shall be presented in a future paper.

The applied LQG/LTR design method provides a powerful robust controller design framework for 9-axes magnetic bearing multi-stage natural gas compressor system. The controller tuning is intuitive for the control engineer and good robustness defined in ISO14893 [3] can be achieved. Future work will focus on more precise specification for the dynamic compliance without relaxing the robustness specification.

The authors would like to thank MAN for providing data used in this paper and for reviewing its contents.

References

[1] A. Masala, R. Shultz, R. Jayawant, “The Move of Active Magnetic Bearings into Upstream Oil & Gas Applications”, Proceedings of the First Brazilian Workshop on Magnetic Bearings, Rio de Janeiro, 2013

[2] R. Somaini, “Comparison of different variable speed compression train configurations with respect to rotordynamic stability and torsional integrity”, Proceedings of the 4st Turbomachinery Symposium, Houston, 2012.

[3] ISO 14839-3: “Mechanical vibration - Vibration of rotating machinery equipped with active magnetic bearings. Part 3 evaluation of stability margin”.

[4] API617: “Axial and Centrifugal Compressors and expander-compressors”. 8th edition.

[5] S. Skogestad, I. Postlethwaite “Multivariable Feedback Control: Analysis and Design”. 2nd Edition, 2005

[6] L. Guzzella, H.P. Geering, "LQG/LTR – Theory for the User", LernModul Nr 19 of Swiss Society for Automatic Control, 2000